第 36 卷 第 2 期 原 子 核 物 理 评 论 Vol. 36, No. 2
2019 年 6 月 Nuclear Physics Review June , 2019

Article ID: 1007-4627(2019) 02-0248-08

First-principles Study of Structural, Mechanical and Thermal Properties of $RE_2Ti_2O_7$ (RE=Gd, Y, Ho, Er)

LIU Huan, LIU Chenguang, YANG Dongyan, XIA Yue, LI Yuhong†

(*School of Nuclear Science and Technology, Lanzhou University, Lanzhou 730000, China*)

Abstract: In this work, we studied the structural, mechanical, and thermal properties of $RE_2Ti_2O_7$ (RE = Gd, Y, Ho, Er) pyrochlores by the first-principles calculations combining with the quasi-harmonic approximation. Our study reveals that $RE_2Ti_2O_7$ possess excellent resistance to compression and shear at the ground state. Moreover, these compounds can be approximate to elastically isotropic materials because their Zener ratios are close to 1. The obtained thermal expansion coefficient agrees well with the experimental results at high temperature. The mean thermal expansion coefficient of the $RE_2Ti_2O_7$ compound is about $(10.4\sim13.1)\times10^{-6}$ K^{-1} in the temperature range of 500∼1 500 K. We also employed Slack's model to estimate thermal conductivity, and the results located in the range of 1.5∼4.9 $W\cdot m^{-1}\cdot K^{-1}$ at 1 000 K.

Key words: rare earth titanate; mechanical property; thermal property; first-principles calculation

CLC number: O38 **Document code:** A **DOI:** 10.11804/NuclPhysRev.36.02.248

1 Introduction

As the worldwide development of nuclear energy continues increasing, successful disposition of the long-lived fission products, such as plutonium and "minor" actinides (Np, Am, and Cm), plays a more and more critical role in the development of advanced nuclear fuel cycles. A prospective approach is that immobilize the high-level radioactive waste (HLW) in host materials[1–5]. The host materials, also called waste form materials, should possess excellent actinides solubility, radiation resistance, and chemical stability. Considering the rugged conditions of the disposal repository (several hundred degrees Celsius and tens of GPa), improved thermal and mechanical stabilities[4] are also required. Thus, a fundamental understanding of the thermal and mechanical properties of the potential forms is essential.

In recent years, compounds with pyrochlore structure are considered to be the most competitive host forms owing to the excellent radiation resistance[1], good stability and durability[6], as well as low leaching rate[5, 7–9]. Plenty of work has been done to reveal the structure[10–12], radiation resistance[1, 12–17], solubility of actinides[18–21], mechanical[10, 22–25] and thermal properties[10, 23–24, 26–36] of pyrochlores. The thermal expansion coefficient (TEC) and thermal conductivity of pyrochlore-type zirconates $RE_2Zr_2O_7$ are reported to be $(8\sim11.8)\times10^{-6}$ K^{-1} and 1.1∼1.5 $W\cdot m^{-1}\cdot K^{-1}$ in the temperature range of 298∼1 500 K respectively[23–24, 29]. The TEC and thermal conductivity of $RE_2Sn_2O_7$ are $(7\sim9)\times10^{-6}$ K^{-1} and 1.8∼2.5 $W\cdot m^{-1}\cdot K^{-1}$ at 1 273 K[34]. These researches suggest that the pyrochlore-type zirconates $RE_2Zr_2O_7$ and stannates $RE_2Sn_2O_7$ possess excellent mechanical and thermal stabilities. However, the mechanical and thermal stabilities of another prospective waste form, titanate, remain to be fully understood.

Liu *et al.*[35–36] presented a study on the thermal conductivity and expansion of the $Gd_2(Ti_xZr_{1-x})_2O_7$ (x=0, 0.25, 0.50, 0.75, 1.00) system. Their researches indicate that thermal conductivity of $Gd_2(Ti_xZr_{1-x})_2O_7$ increases with increasing Ti content, the TEC of $Gd_2(Ti_xZr_{1-x})_2O_7$ decreases with increasing Ti content at the same temperature. Moreover, the elastic modulus and thermal conductivity of $RE_2T_2O_7$ (T=Ge, Ti, Sn, Zr, Hf) are also significantly influenced by the change of T[33, 37]. On this basis, one can infer that the mechanical and thermal properties of titanates are significantly different from those

Received date: 19 Sep. 2018; **Revised date:** 5 Mar. 2019

Foundation item: National Natural Science Foundation of China (11775102)

Biography: LIU Huan(1990–), female, Longxian, Shaanxi, Ph.D. student, working on high level nuclear wastes immobilization; E-mail: liuhuan14@lzu.edu.cn

† **Corresponding author:** LI Yuhong, E-mail: liyuhong@lzu.edu.cn.

of zirconates. Recently Dong *et al.*[38] carried out a molecular dynamics (MD) simulations on a series of $A_2B_2O_7$ (A=Lu, Yb, Er, Y, Gd, Eu, Sm, Nd, Ce, La; B=Ti, Ru, Mo, Sn, Zr, Pb, Ce) pyrochlores, and estimated their bulk modulus, average heat capacity, and TEC. However, a systematic and comprehensive study of the mechanical and thermal properties of $RE_2Ti_2O_7$ titanate pyrochlores at *ab initio* level with higher accuracy is still needed.

In this work, the density functional theory (DFT) is employed to calculate the structural and mechanical properties of $RE_2Ti_2O_7$ (RE=Gd, Y, Ho, Er) pyrochlores at ground-state, which including lattice parameter, elastic constants, and elastic modulus. In order to obtain the thermal properties, lattice vibration, TEC, heat capacity, and thermal conductivity were also computed within quasi-harmonic approximation (QHA).

2 Computational details

The first-principles calculations based on DFT are performed with the Vienna Ab initio Simulation Package (VASP)[39]. The projector augmented wave (PAW) method[40] is employed to describe the interaction between ions and electrons. The GGA-PW91 scheme[41] for the exchange-correlation potential is used. The *f*-electrons of Gd, Ho, and Er are frozen in the core. A conventional cubic unit cell containing 88 atoms is chosen as the initial models throughout our work. The crystal structures are fully relaxed using a quasi-Newton algorithm. The cutoff energy is set to 450 eV. The special points sampling integrations in Brillouin zone based on the Monkhorst-Pack method is 2×2×2. The relaxation of the electronic degrees of freedom is stopped when the total energy change between two steps is smaller than 10^{-8} eV· atom $^{-1}$. The ionic relaxation is stopped when all forces were smaller than 10^{-5} eV·Å^{-1}. The Hubbard-U correction is not employed in the present work as the previous works[32, 34] have confirmed that the Hubbard-U correction can hardly improve the accuracy of thermal properties.

Base on the density functional perturbation theory (DFPT)[42], the force constants in real-space are calculated by VASP. The phonon frequencies are calculated using PHONOPY[43]. We repeat the above computations at 10 volume points to obtain the temperature response of lattice parameters within quasi-harmonic approximation (QHA)[44].

3 Results and discussion

3.1 Structural properties

Pyrochlore is a derivative of the fluorite (MO_2). The structures of pyrochlore and fluorite are illustrated in Fig. 1. The pyrochlore has a cubic structure with eight molecules in an ideal unit cell (Z=8), and the space group is $Fd\bar{3}m$. For titanates, larger RE^{3+} cations are at 16*d* $\left(\frac{1}{2}, \frac{1}{2}, \frac{1}{2}\right)$ site, smaller Ti^{4+} cations are at 16*c* (0, 0, 0) site, O^{2-} anions occupy 48*f* $\left(x, \frac{1}{8}, \frac{1}{8}\right)$ and 8*b* $\left(\frac{3}{8}, \frac{3}{8}, \frac{3}{8}\right)$ positions. The crystal structures are fully optimized by DFT calculations, and the relaxed lattice constants (a) and 48*f* position parameters (x) are presented in Table 1. Experimental values[3, 12, 45] are also listed for comparison. Compared with other calculations[46–47] our calculation results are the most consistent with experiments.

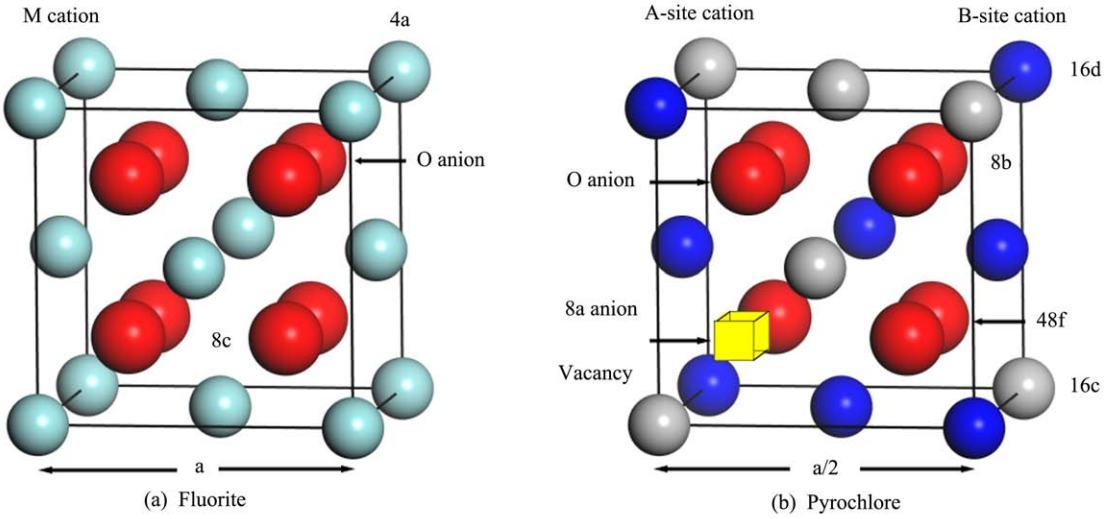

Fig. 1　(color online) Crystal structures of (a) ideal fluorite (MO_2; M=cation) and (b) pyrochlore ($A_2B_2O_7$; A, B=cations).

Table 1 Calculated lattice parameters and bond lengths for $RE_2Ti_2O_7$ (RE = Gd, Y, Ho, Er) pyrochlore. The values in parentheses indicate the percent error (%) relative to the experimental value in Ref. [12].

RE	a/Å	x/Å	$d_{Re-O'}$/Å	d_{Re-O}/Å	d_{Ti-O}/Å	∠TiOTi/(°)
Gd (this work)	10.140 9 (0.44)	0.329 8 (1.07)	2.195 6 (0.43)	2.488 3 (1.41)	1.967 0 (0.31)	131.392 0
Gd (cal. Ref. [47])	10.020 7 (1.62)	0.329 1 (0.86)	2.169 5 (1.16)	2.464 0 (2.38)	1.941 0 (1.02)	131.789 0
Gd (cal. Ref. [46])	10.206 0 (0.20)	0.329 2 (0.89)		2.509 0 (0.59)	1.977 0 (0.82)	
Gd (exp. Ref. [12])	10.186 0	0.326 3	2.205 0	2.524 0	1.961 0	
Gd (exp. Ref. [45])	10.182 0	0.327 0				
Gd (exp. Ref. [3])	10.185 0	0.322 0				
Y (this work)	10.097 9 (0.02)	0.330 8 (0.24)	2.186 3 (0.03)	2.471 3 (0.23)	1.962 5 (0.93)	130.899 4
Y (cal. Ref. [47])	9.967 9 (1.31)	0.331 5 (0.45)	2.158 0 (1.33)	2.435 0 (1.70)	1.940 0 (1.02)	130.510 0
Y (cal. Ref. [46])	10.200 0 (0.99)	0.329 7 (0.09)		2.632 0 (6.26)	1.978 0 (0.92)	
Y (exp. Ref. [12])	10.100 2	0.330 0	2.187 0	2.477 0	1.960 0	
Ho (this work)	10.055 2 (0.48)	0.332 1 (1.10)	2.177 0 (0.46)	2.451 4 (1.51)	1.959 9 (0.30)	130.172
Ho (cal. Ref. [47])	9.930 6 (1.72)	0.331 5 (0.91)	2.150 0 (1.69)	2.426 0 (2.53)	1.933 0 (1.07)	130.520 0
Ho exp. Ref. [12])	10.104 1	0.328 5	2.187 0	2.489 0	1.954 0	
Er (this work)	10.029 6 (0.49)	0.332 8 (1.53)	2.171 5 (0.48)	2.440 2 (1.92)	1.958 0 (0.62)	129.789 8
Er (cal. Ref. [47])	9.902 8 (1.75)	0.332 2 (1.34)	2.144 0 (1.74)	2.414 0 (2.97)	1.931 0 (1.77)	130.120 0
Er (cal. Ref. [46])	10.119 0 (0.40)	0.331 8 (1.22)		2.469 0 (0.76)	1.971 0 (1.28)	
Er (exp. Ref. [12])	10.078 7	0.327 8	2.182 0	2.488 0	1.946 0	

3.2 Mechanical properties

The mechanical properties of $RE_2Ti_2O_7$ are studied by analyzing their elastic constants and elastic modulus. DFPT calculations are performed based on the full relaxed structure to obtain the elastic constants. Elastic modulus, including bulk modulus B, shear modulus G, Young's modulus E, and Poisson's ratio μ are then evaluated from the elastic constants using the Voigt-Reuss-Hill approximation[48]. The results are shown in Table 2. In a cubic structure crystal, only three of the elastic constants are independent of each other, *i.e.*, C_{11}, C_{12}, and C_{44}. C_{11} is the uniaxial deformation along the [001] direction; C_{12} represents the pure shear stress along [110] direction at (110) crystal plane; C_{44} is a pure shear deformation on (100) crystal plane. For all these compounds, C_{11} is almost three times as large as C_{12} or C_{44}, and $C_{44} < C_{12}$ which deviations from the Cauchy relation indicating that the interatomic forces of $RE_2Ti_2O_7$ are non-central and angle-dependent[49]. The shear resistance of $RE_2Ti_2O_7$ is relatively weaker than the compression resistance because the shear modulus of a cubic crystal is strongly determined by C_{44}.

For all $RE_2Ti_2O_7$ compounds, the bulk modulus smaller than 200 GPa, which are consistent with previous theoretical studies (186.91 GPa for $Gd_2Ti_2O_7$, 189.83 GPa for $Ho_2Ti_2O_7$, 191.00 GPa for $Er_2Ti_2O_7$)[50]. The Poisson′s ratio (μ) of $RE_2Ti_2O_7$ (RE=Gd, Y, Ho, Er) compounds is about 0.25, which meets the typical Poisson's ratio value of ceramics (0.2∼0.3) well. The Zener anisotropy ratio Z=2C_{44}/(C_{11}- C_{12}) is a parameter used to characterize the elastic anisotropy of a cubic structure (where Z=1 means isotropic)[51]. Our results indicate that $RE_2Ti_2O_7$ are almost elastically isotropic but slightly stiffer along the [100] direction than along [111] (the maximum Young's modulus is along [100])[37]. According to our calculations, the elastic modulus of $RE_2Ti_2O_7$(RE=Gd, Y, Ho, Er), including bulk modulus, Young′s modulus, and shear modulus, are larger than that of zirconates $RE_2Zr_2O_7$(RE=La-Gd)[22–24], which indicates that titanates possess more excellent mechanical stability than zirconates do.

Table 2 Calculated values of elastic constants (in GPa), *i.e.*, C_{11}, C_{12}, C_{44}, bulk modulus B (GPa), shear modulus G (GPa), Young′s modulus E (GPa), Poisson's ratio μ, Zener anisotropy ratio Z, density ρ (g/cm^3), longitudinal (ν_l), transverse (ν_τ) and average (ν_m) sound wave velocity (m/s), Debye temperature Θ (K).

	RE^{3+} /nm	RE^{3+} /Ti^{4+}	C_{11}	C_{12}	C_{44}	B	G	E	μ	Z	ρ	v_l	v_t	v_m	Θ
$Gd_2Ti_2O_7$	1.053	1.740 5	329.156	116.956	95.549	187.689	99.639	253.973	0.262	0.901	6.565	6 987.539	3 895.798	5 327.207	587.392
$Y_2Ti_2O_7$	1.019	1.684 3	329.322	113.798	92.003	185.640	98.013	250.035	0.257	0.854	4.991	7 961.080	4 431.472	6 061.133	671.159
$Ho_2Ti_2O_7$	1.015	1.677 7	338.725	111.859	93.335	187.481	100.914	256.688	0.248	0.823	6.928	6 817.839	3 816.565	5 215.734	579.998
$Er_2Ti_2O_7$	1.004	1.659 5	343.732	114.049	94.576	190.610	102.221	260.156	0.249	0.824	7.042	6 813.375	3 809.965	5 207.550	580.568

3.3 Phonon dispersion curves and density of states

The calculated phonon dispersion curves and the density of states (DOS) for $RE_2Ti_2O_7$ (RE=Gd, Y, Ho, Er) are presented in Fig. 2. It is found that $RE_2Ti_2O_7$ pyrochlores with different RE elements show similar shapes of the phonon dispersion curves and DOS. Besides, in the range of 1 to 3 THz, some optical branches are overlapping with the acoustic branches. According to Lan's research[33], the low-lying optical phonon branches will reduce the lattice thermal conductance significantly.

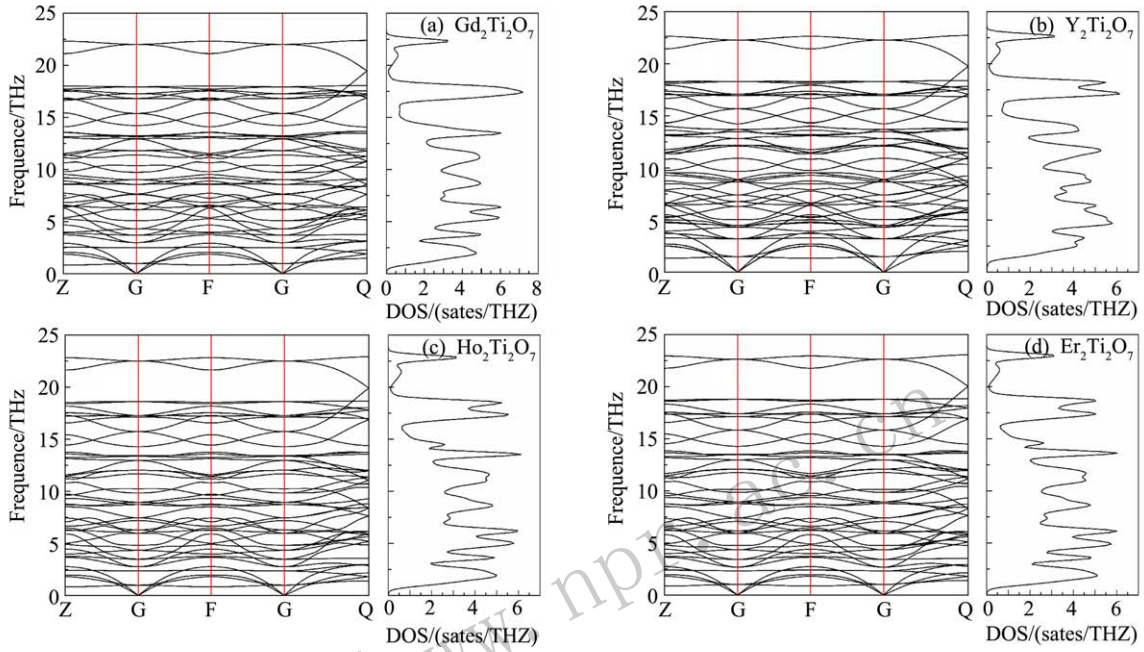

Fig. 2　(color online) Phonon dispersions and density of states (DOS) for $RE_2Ti_2O_7$ (RE=Gd, Y, Ho, Er) pyrochlores.

Fig. 3 shows the partial density of states (PDOS) of $RE_2Ti_2O_7$ (RE=Gd, Y, Ho, Er). It is clear that the acoustic branches and low-lying optical branches are primarily ascribed to the vibrations of RE^{3+} cations. Moreover, the DOS of RE^{3+} cations become higher and narrower with the increase of atomic mass. This

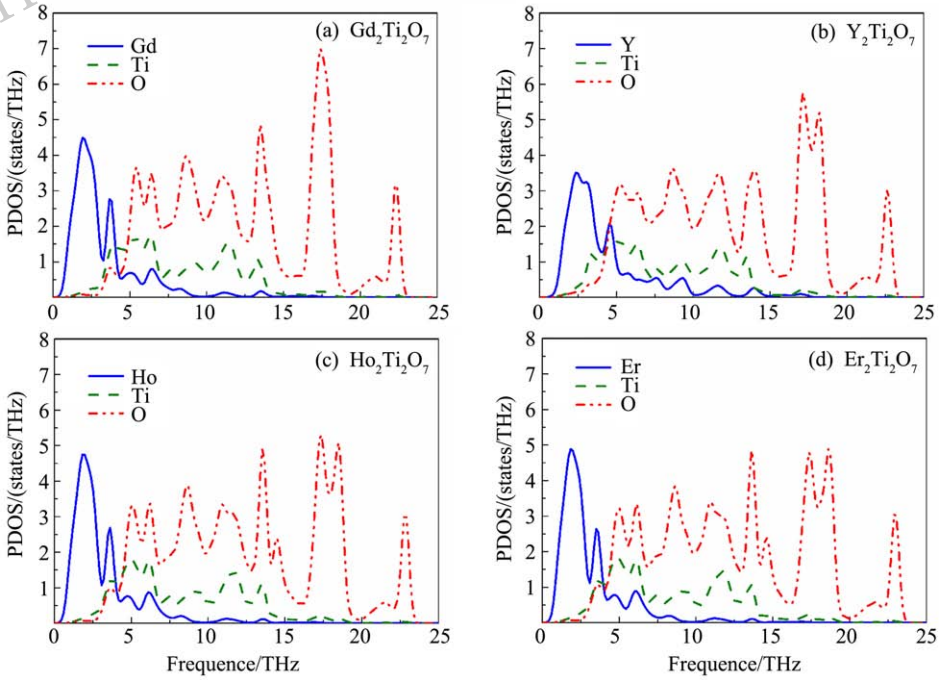

Fig. 3　(color online) Partial density of states (PDOS) for $RE_2Ti_2O_7$ (RE=Gd, Y, Ho, Er) pyrochlores.

result comes from the fact that the heavier atom generally exhibits lower vibration frequency. The DOS of Y^{3+} in the low-frequency region (1∼5 THz) shows a different shape with that of other RE^{3+} because of its different electron configuration. The optical branches are ascribed to the vibrations of Ti^{4+} and O^{2-}. The DOS corresponding to Ti^{4+} is statistically invariant, which suggests that the bonding environment around Ti^{4+} remains unchanged in different compounds. While the DOS of O^{2-} become shallower with decreasing RE cation radius gradually.

3.4 Thermal properties

TEC is a critical evaluation criterion to assess the thermal stability of the HLW form materials. We calculated the TEC of $RE_2Ti_2O_7$ from 0 to 1 500 K using the quasi-harmonic approximation. The volumetric thermal expansion coefficient is given by

$$\alpha_V(T) = \frac{1}{V}\left(\frac{\partial V}{\partial T}\right) \tag{1}$$

and the linear thermal expansion is described as

$$\alpha_l(T) = \frac{1}{L}\left(\frac{\partial L}{\partial T}\right) . \tag{2}$$

For cubic structure, $\alpha_V \approx 3\alpha_l$. Fig. 4. illustrate the volumetric thermal expansion coefficients of $RE_2Ti_2O_7$ (RE=Gd, Y, Ho, and Er). It is evident that the obtained TEC of $Gd_2Ti_2O_7$ is in good agreement with the experimental results at high temperature, but is higher at low temperature[36]. The mean TEC of $RE_2Ti_2O_7$ compounds is about $(10.4\sim13.1)\times10^{-6}K^{-1}$ in the temperature range 500∼1 500 K, which is higher than that of $RE_2Zr_2O_7$. Among the investigated compounds, $Er_2Ti_2O_7$possesses the smallest TEC, while $Y_2Ti_2O_7$ possesses the largest.

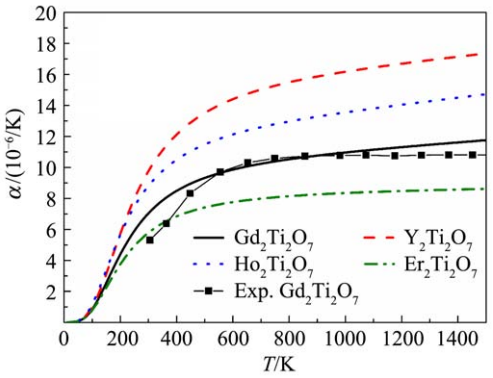

Fig. 4 (color online) The temperature dependence of TEC for $RE_2Ti_2O_7$ (RE=Gd, Y, Ho, Er) pyrochlores. The experiment values of $Gd_2Ti_2O_7$ were obtained from Ref. [36].

The calculated heat capacity at constant pressure (C_P) and constant volume (C_V) are presented in Fig. 5. C_V almost equals C_P at the lower temperature range and follows T^3 power-law. At high temperature, C_V approaches the Dulong-Petit limit and converges towards $3Nk_B$, whereas the C_P increases continuously. The difference between C_V and C_P at high tempera-

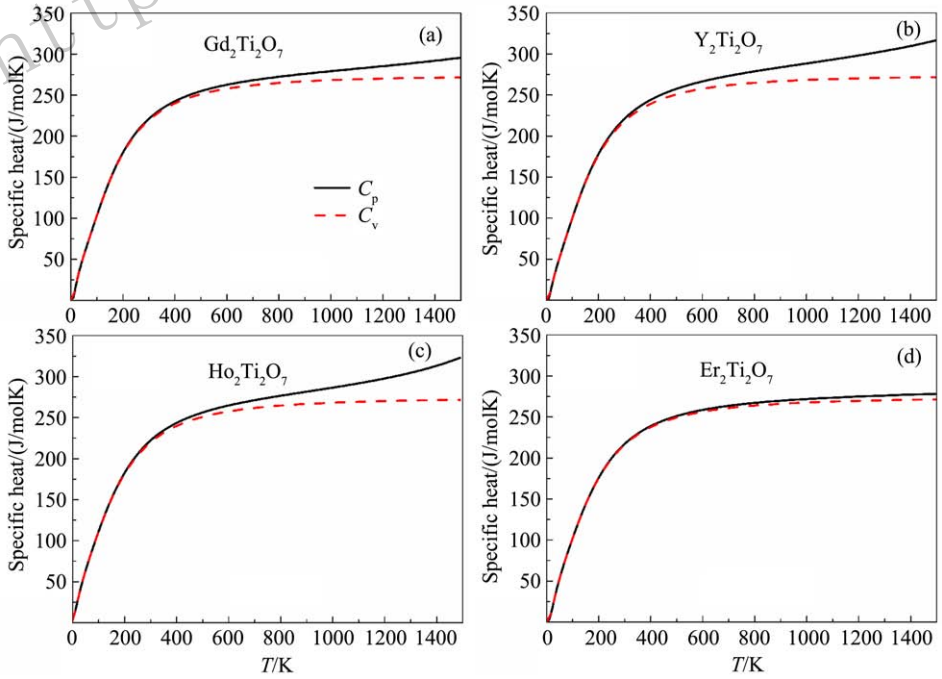

Fig. 5 (color online) The temperature dependence of heat capacity at constant volume (C_V) and pressure (C_P) for $RE_2Ti_2O_7$ (RE=Gd, Y, Ho, Er) pyrochlores.

ture origins from thermal expansion ($C_P - C_V = \alpha_V^2 V(T)$TB, where $V(T)=(1+\alpha_V T)V$ is the equilibrium cell volume at temperature T). Simultaneously, the heat capacities of $RE_2Ti_2O_7$ are smooth, showing no evidence of phase transitions over the temperature range from 0∼1 500 K.

The intrinsic thermal conductivity at a specific temperature is calculated with the following equation proposed by Slack.[52]

$$\kappa = A\frac{\bar{M}\theta^3\delta}{\gamma^2 n^{3/2}T}\ , \tag{3}$$

γ represents the Grüneisen parameter which can be used to characterize the anharmonicity of crystals, $A \approx 3.1\times10^{-6}$, n is the number of atoms in the primitive unit cell, δ^3 is the volume per atom in Å^3, $\bar{M}$ represents the average mass of the atoms in the crystal in amu, and Θ is the Debye temperature which is presented in Table 2. The Debye temperature can be estimated using the following equations[53]:

$$\theta = \frac{hv_m}{k_B}\left(\frac{3N_0}{4\pi V}\right)^{1/3}, \tag{4}$$

$$\frac{1}{v_m^3} = \frac{1}{3}\left(\frac{1}{v_l^3}+\frac{2}{v_t^3}\right), \tag{5}$$

$$\begin{cases} l = \sqrt{\left(B+\frac{3}{4}G\right)\rho} \\ v_t = \sqrt{\frac{G}{\rho}} \end{cases}, \tag{6}$$

where N_0 is the number of atoms; h is Plank constant, k_B is Boltzmann constant; ν_l, ν_t, and ν_m are the longitudinal, transverse and average sound velocity, respectively; and ρ is the theoretical density. This model assumes that optical modes do not contribute to the heat transport processes. In addition, the only type of phonon scattering mechanism considered in this model is anharmonic Umklapp scattering.

The theoretical thermal conductivity of $RE_2Ti_2O_7$ estimated using Eq. (3) is shown in Fig. 6. The thermal conductivity decreases with the increase of temperature, which can be attributed to the phonon-phonon Umklapp scattering. When the phonon mean free path is reduced to the minimum value, which equivalents to the average distance between two atoms in the crystal, the thermal conductivity achieves minimal. Comparing the calculated thermal conductivity of $Gd_2Ti_2O_7$ to the experimental results[35], one can note that it is significantly overestimated at low temperature(lower than Debey temperature) but underestimated at very high temperature(>1 300K). In fact, the Slack′s model cannot correctly describe the thermal conductivity at low temperature because of the following two reasons: Firstly, in this model, the phonon mean free path is regarded as the mean atomic distance in the whole temperature range. Actually, the assumed value of phonon mean free path is significantly smaller than the actual phonon mean free path in the temperature range below the Debye temperature. Secondly, as mentioned in Sec. 3.3, low-lying optical branches which lie in the acoustic range can significantly change the lattice thermal conductivity[33]. While in this model, the optical phonon is ignored. However, our calculated thermal conductivity in the range of 1 000 to 1 200 K is valuable. The thermal conductivity of $Gd_2Ti_2O_7$, $Y_2Ti_2O_7$, $Ho_2Ti_2O_7$, and $Er_2Ti_2O_7$ at 1 000 K is 2.4, 1.5, 1.5, and 4.9 W·m^{-1}·K^{-1}, respectively. There is no doubt that further work with more depth is required to reveal the failure of this work, and a more advanced model is needed to predict the thermal conductivity correctly.

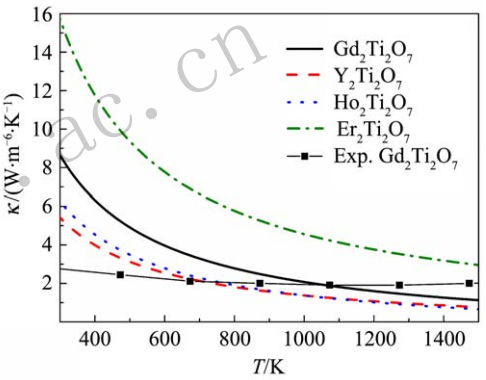

Fig. 6 (color online) The theoretical thermal conductivity of $RE_2Ti_2O_7$ compounds. The experiment values of $Gd_2Ti_2O_7$were obtained from Ref. [35]. The error bars of cited experimental data are omitted because they are smaller than the symbols.

4 Conclusion

The structural, mechanical, and thermal properties of titanate pyrochlores $RE_2Ti_2O_7$(RE=Gd, Y, Ho, Er) are studied by first-principles calculations. The relaxed structural parameters show a good agreement with the reported experiments. The calculated elastic constants and elastic modulus indicate that $RE_2Ti_2O_7$ (RE = Gd, Y, Ho, and Er) are mechanically stable and can be approximate to elastically isotropic (slightly stiffer along [100] axes) at the ground state. By applying quasi-harmonic approximation, their thermal expansion coefficient, heat capacity, and thermal conductivity at different temperatures are calculated. The calculated thermal expansion coefficient of $Gd_2Ti_2O_7$ is in excellent agreement with the available experiments at high temperature. The mean TEC of $RE_2Ti_2O_7$ compounds is about $(10.4\sim13.1)\times10^{-6}$ K^{-1} in the

temperature range of 500∼1 500 K. The thermal conductivity of $RE_2Ti_2O_7$ (RE=Gd, Y, Ho, Er) compounds is in the range of 1.5∼4.9 $W\cdot m^{-1}\cdot K^{-1}$ at 1 000 K.

In summary, $RE_2Ti_2O_7$(RE=Gd, Y, Ho, Er) pyrochlores exhibit more outstanding mechanical stability than $RE_2Zr_2O_7$ due to they have higher compression resistance and shear resistance. For $RE_2Ti_2O_7$(RE=Gd, Y, Ho, Er), $Er_2Ti_2O_7$ has the largest elastic module, the lowest thermal expansion coefficient, and the highest thermal conductivity, so it is more suitable for immobilization of high-level radioactive waste.

References:

[1] EWING R C. J Appl Phys, 2004, **95**: 5949.
[2] EWING R C, LUTZE W. Ceram Int, 1991, **17**: 287.
[3] SUBRAMANIAN M A, ARAVAMUDAN G, SUBBA RAO G V. Prog Solid State Chem, 1983, **15**: 55.
[4] HENCH L L, CLARK D E, CAMPBELL J. Nucl Chem Waste Manag, 1984, **5**: 149.
[5] KAMIZONO H, HAYAKAWA I, MURAOKA S. J Am Ceram Soc, 1991, **74**: 863.
[6] WEBER W J, NAVROTSKY A, STEFANOVSKY S, *et al.* MRS Bull, 2011, **34**: 46.
[7] HAYAKAWA I, KAMIZONO H. J Nucl Mater, 1993, **202**: 163.
[8] HAYAKAWA I, KAMIZONO H. J Mater Sci, 1993, **28**: 513.
[9] HAYAKAWA I, KAMIZONO H. MRS Proc, 2011, **257**: 257.
[10] FENG J, XIAO B, WAN C L, *et al.* Acta Mater, 2011, **59**: 1742.
[11] CHEN Z J, XIAO H Y, ZU X T, *et al.* Comput Mater Sci, 2008, **42**: 653.
[12] LIAN J, CHEN J, WANG L M, *et al.* Phys Rev B, 2003, **68**: 134107.
[13] LUMPKIN G R. Elements, 2006, **2**: 365.
[14] SICKAFUS K E. Science (80), 2000, **289**: 748.
[15] WANG S X, BEGG B D, WANG L M, *et al.* J Mater Res, 2011, **14**: 4470.
[16] LIAN J, WANG L, CHEN J, *et al.* Acta Mater, 2003, **51**: 1493.
[17] SICKAFUS K E, GRIMES R W, VALDEZ J A, *et al.* Nat Mater, 2007, **6**: 217.
[18] LANG M, ZHANG F X, EWING R C, *et al.* J Mater Res, 2011, **24**: 1322.
[19] LANG M, ZHANG F, ZHANG J, *et al.* Nucl Instr and Meth B, 2010, **268**: 2951.
[20] LIAN J, EWING R C, WANG L M, *et al.* J Mater Res, 2011, **19**: 1575.
[21] SATTONNAY G, MOLL S, THOMÉ L, *et al.* Nucl Instr and Meth B, 2012, **272**: 261.
[22] MORIGA T, YOSHIASA A, KANAMARU F, *et al.* Solid State Ionics, 1989, **31**: 319.
[23] VASSEN R, CAO X, TIETZ F, *et al.* J Am Ceram Soc, 2004, **83**: 2023.
[24] WU J, WEI X. Slack's model estimated the thermal conductivity N P, *et al.* J Am Ceram Soc,2004, **85**: 3031.
[25] PRUNEDA J M, ARTACHO E. Phys Rev B,2005, **72**: 085107.
[26] SURESH G, SEENIVASAN G, KRISHNAIAH M V, *et al.* J Nucl Mater, 1997, **249:** 259.
[27] LUTIQUE S, KONINGS R J M, RONDINELLA V V, *et al.* J Alloys Compd, 2003, **352**: 1.
[28] LUTIQUE S, JAVORSKÝ P, KONINGS R J M, *et al.* J Chem Thermodyn, 2003, **35**: 955.
[29] LEHMANN H, PITZER D, PRACHT G, *et al.* J Am Ceram Soc, 2003, **86**: 1338.
[30] BANSAL N P, ZHU D. Mater Sci Eng A, 2007, **459**: 192.
[31] LIU Z G, OUYANG J H, ZHOU Y. J Alloys Compd, 2009, **472**: 319.
[32] FENG J, XIAO B, ZHOU R, *et al.* Scr Mater, 2013, **68**: 727.
[33] LAN G, OUYANG B, SONG J. Acta Mater, 2015, **91**: 304.
[34] FENG J, XIAO B, ZHOU R, *et al.* Scr Mater, 2013, **69**: 401.
[35] LIU Z G, OUYANG J H, ZHOU Y, *et al.* Mater Lett, 2008, **62**: 4455.
[36] LIU Z G, OUYANG J H, ZHOU Y, *et al.* Mater Des, 2009, **30**: 3784.
[37] LIU B, WANG J Y, LI F Z, *et al.* Acta Mater, 2010, **58**: 4369.
[38] DONG L, LI Y, DEVANATHAN R, *et al.* RSC Adv, 2016, **6**: 41410.
[39] KRESSE G, FURTHMÜLLER J. Comput Mater Sci, 1996, **6**: 15.
[40] BLÖCHL P E. Phys Rev B, 1994, **50**: 17953.
[41] PERDEW J P, JACKSON K A, PEDERSON M R, *et al.* Phys Rev B, 1992, **46**: 6671.
[42] BARONI S, DE GIRONCOLI S, DAL CORSO A. Rev Mod Phys, 2001, **73**: 515.
[43] TOGO A, OBA F, TANAKA I. Phys Rev B, 2008, **78**: 134106.
[44] DAVIES G F. J Phys Chem Solids, 1973, **34**: 1417.
[45] TABIRA Y, WITHERS R L, MINERVINI L, *et al.* J Solid State Chem, 2000, **153**: 16.
[46] ZHANG Z L, XIAO H Y, ZU X T, *et al.* J Mater Res, 2011, **24**: 1335.
[47] KUMAR S, GUPTA H C. Vib Spectrosc, 2012, **62**: 180.
[48] NYE J F. Physical Properties of Crystals: Their Representation by Tensors and Matrices[M]. United states, Oxford University Press Inc, 1985: 351.
[49] WONG J, KRISCH M, FARBER D L, *et al.* Phys Rev B, 2005, **72**: 064115.
[50] LIU C G, CHEN L J, YANG D Y, *et al.* Comput Mater Sci, 2016, **114**: 233.
[51] INGEL R P, III D L. J Am Ceram Soc, 1988, **71**: 265.
[52] SLACK G A. Solid State Phys, 1979, **34**: 1.
[53] KITTEL C. Introduction to Solid State Physics[M] 8th Ed. New Jersey: John Wiley & Sons, 2004: 114.

$RE_2Ti_2O_7$(RE=Gd, Y, Ho, Er)的结构、机械性能及热学性质的第一性原理研究

刘 焕，刘晨光，杨冬燕，夏 月，李玉红†

（兰州大学核科学与技术学院，兰州 730000）

摘要： 本文利用第一性原理和准谐近似的方法研究了一系列钛酸盐烧绿石，即$RE_2Ti_2O_7$ (RE = Gd, Y, Ho,Er)的结构、机械性能及热学性质。研究结果表明，在基态下$RE_2Ti_2O_7$具有良好的抗压、抗剪切能力。并且，由于这些化合物的齐纳指数接近于1，可近似地看作各向同性材料。此外，计算得到的热膨胀系数在高温区与实验值符合得较好。在500~1 500 K温度区间内，平均热膨胀系数为$(10.4\sim13.1)\times10^{-6}$ K^{-1}。基于Slack模型，我们还计算了这些材料的晶格热导率，当温度等于1 000 K时，这四种物质的热导率在区间(1.5~4.9) $W\cdot m^{-1}\cdot K^{-1}$内。

关键词： 稀土钛酸盐；机械性能；热学性质；第一性原理

收稿日期： 2018-09-19；　**修改日期：** 2019-03-05

基金项目： 国家自然科学基金资助项目(11775102)

† **通信作者：** 李玉红，E-mail: liyuhong@lzu.edu.cn。